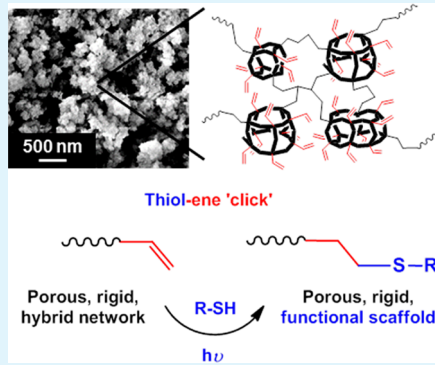


Conceptual Design of Large Surface Area Porous Polymeric Hybrid Media Based on Polyhedral Oligomeric Silsesquioxane Precursors: Preparation, Tailoring of Porous Properties, and Internal Surface Functionalization

Filipa Alves,[†] Pascal Scholder,[†] and Ivo Nischang*

Institute of Polymer Chemistry, Johannes Kepler University Linz, Welser Str. 42, A-4060 Leonding, Austria

ABSTRACT: We report on the preparation of hybrid, organic–inorganic porous materials derived from polyhedral oligomeric vinylsilsesquioxanes (vinylPOSS) via a single-step molding process. The monolithic, large surface area materials are studied with a particular focus on morphology and porous properties. Radical vinyl polymerization of the nanometer-sized POSS building blocks is therefore utilized via a thermally initiated route and in porogenic diluents such as tetrahydrofuran and polyethylene glycols of varying composition. Careful choice of these porogenic solvents and proper choice of initiator concentration lead to highly porous monolithic building entities which show a rigid, 3D-adhered, porous structure, macroscopically adapting the shape of a given mold. The described materials reflect Brunauer–Emmett–Teller (BET) surface areas of 700 m²/g or more and maximum tunable mesopore volumes of up to 2 cm³/g. Experimental investigations demonstrate the option to tailor nanoporosity and macroporosity in the single-step free-radical polymerization process. While studies on the influence of the used porogenic solvents reveal tuneability of pore sizes due to the unique pore formation process, tailored existence of residual vinyl groups allows facile postpolymerization modification of the highly porous, large surface area hybrid materials exploited via thiol–ene “click” chemistry. Our developed, simply realizable preparation process explores a new route to derive porous organic–inorganic hybrid adsorbents for a wide variety of applications such as extraction, separation science, and catalysis.



KEYWORDS: *hierarchical pore structure, hybrid materials, porous properties, nanohybrid building blocks, polyhedral oligomeric silsesquioxane (POSS), thiol–ene “click” chemistry*

1. INTRODUCTION

Adsorbents with tailorable porous structures have a wide variety of applications including storage of gases,¹ catalytic reactors,^{2–7} permeation-selective membranes,^{8,9} and as selective adsorbers for specific compounds,^{10,11} as well as in liquid chromatographic applications.^{12,13} For the derivation of porous entities, based on organic precursors and cross-linking polymerization systems several methods to tailor in particular nanoporous (micro- and mesoporous) and macroporous properties can be found to be state-of-the art.^{14–20}

Methods of tailoring the porous properties of polymeric bead-based and monolithic adsorbents typically use free-radical polymerization and rely on the choice of monomeric precursors, including monomers and cross-linkers, their relative concentration, choice of initiator, and source of initiation, e.g., thermally or photochemically.^{14–20} An often employed method of tuning the porous properties of monolithic materials derived from *in situ* polymerization exploits porogenic diluents. These have characteristic solvating properties for the monomeric precursors and also the cross-linked polymers that form. The worse solvating properties of the porogenic diluents vs formed polymeric materials lead to phase separation and pore formation within the time scale of polymerization.^{14,16,19}

It is generally accepted that in the formation of porous monolithic entities phase separation is a direct result of the worse solvating properties of polymeric material in porogenic diluents in the closed mold. The result is a porous, 3D, cross-linked material. With an appropriate tuning of macroporous properties, such monolithic materials have a wide variety of flow-through applications, excellent integrative features, and are the materials of choice for related engineering applications. This, to the majority includes liquid chromatographic separations,¹⁹ extraction of components of interest,¹⁰ or as scaffolds for immobilizing reactive or catalytic moieties.²

In our search for porous adsorbents that combine the desirable properties of a permanent high surface area, porous structure as found in silica-based monoliths,¹³ but also having accessibility in a variety of engineering formats as for polymer-based scaffolds,^{2,19} we have pursued the use of monolithic adsorbents based on a vinylsilsesquioxane cage mixture (vinylPOSS).²⁰ Preliminary experiments showed that such precursors facilitate accessibility of a large, dry-state surface area

Received: December 10, 2012

Accepted: March 14, 2013

Published: March 14, 2013

of up to $900 \text{ m}^2/\text{g}$ under the specific preparatory conditions.²⁰ The material was prepared by using a single-phase liquid polymerization mixture composed of a vinylPOSS monomer, initiator, and porogenic diluent.

The synthesis of polyhedral oligomeric silsesquioxanes and their chemical decoration with desirable pendant functionality is well-known.²¹ Materials based thereon are increasingly finding applications ranging from dendritic materials to high performance polymers^{21–23} but also for the preparation of nanocomposites using a variety of explored linking chemistries.^{24–28} Porous materials based on such types of hybrid nanobuilding blocks historically have been prepared via different methodologies, e.g., via thermolysis, copper-mediated coupling, and hydrosilation methods allowing the preparation of materials exhibiting interesting porous properties.^{29–43} For example, the Laine group being quite active in this area has prepared porous materials by hydrosilylative copolymerization of equimolar amounts of hydrido- and vinylsilsesquioxanes under catalytic conditions with platinum divinyltetramethyldisiloxane.³⁰ Preparation of this material was performed in a stirred reaction vessel. This process eventually resulted in a gel which on vacuum drying showed shrinkage and appeared as a brittle glassy solid. Nitrogen sorption gave Brunauer–Emmett–Teller (BET) surface areas of 380 – $530 \text{ m}^2/\text{g}$ with “observable” pore volumes of 0.19 – $0.25 \text{ cm}^3/\text{g}$. The Morris group showed that POSS-containing polymers can be prepared using hydrosilation reactions to produce materials with a mesoporous structure. Polymers with longer organic linkages were synthesized.³² This approach indicated a more “flexible” structure. Other examples include Sonogashira cross-coupling involving copper(I) and palladium catalytic systems resulting in materials of surface areas up to $1042 \text{ m}^2/\text{g}$ and maximum pore volumes of $0.87 \text{ cm}^3/\text{g}$.³⁷ The authors also discussed that the efficiency in cross-linking strongly influences the length and connectable sites of the ethynyl bridges, influencing the BET surface areas and the micropore size distributions of these materials. More recently, Qin et al.⁴¹ prepared a covalently linked microporous organic–inorganic hybrid material containing POSS structural elements using Schiff base chemistry adding to the toolbox of the preparation of this type of porous material. The apparent surface area, calculated after the BET model, was $283 \text{ m}^2/\text{g}$, and a mesopore volume of $0.226 \text{ cm}^3/\text{g}$ was achieved. Polyimide aerogels cross-linked through amine-functionalized polyoligomeric silsesquioxanes showed flexibility, very low density, and yet surface areas of 230 – $280 \text{ m}^2/\text{g}$.⁴³

While the exploration of linking reactions in the preparation of hybrid porous materials based on POSS is an area of continuous growth, only a few recent approaches demonstrate the preparation of monolithic materials showing features that allow their later engineering applications involving flow-through.^{20,44} Such challenge may be addressed by creating such types of materials *in situ* and in a single step within the confines of suitable molds, using straightforward and simple approaches such as free-radical polymerization. In view of the previous attempts to create large surface area materials and detail their porous properties, such an approach is rarely reported.²⁰ However, it may allow adaptation to a variety of research laboratories to be explored for potential definite-purpose applications.

The current study explores the accessibility of porous adsorbent media based on thermally initiated free-radical polymerization of a vinylPOSS cage mixture. We study in detail the impact of binary porogenic solvent compositions,

including macroporogenic and microporogenic constituents and initiator concentration, enabling preparation of rigid structures via the number of alkyl linkages between the individual precursors and their formed assemblies, respectively, microscopic structures. Consequently, accessible nanoporous (in particular mesoporous) and macroporous properties are studied in detail. Under essentially all conditions, the materials can be prepared with large surface areas despite the successful tailoring of macroporous properties in a single step. Following the discussion of the tailoring of properties on different length and morphological scales, we access and demonstrate in detail a facile route to provide an interface modification of these porous materials via thiol–ene “click” chemistry. This approach provides not only efficient surface decoration but also molecularly defined interface chemistry.

2. EXPERIMENTAL SECTION

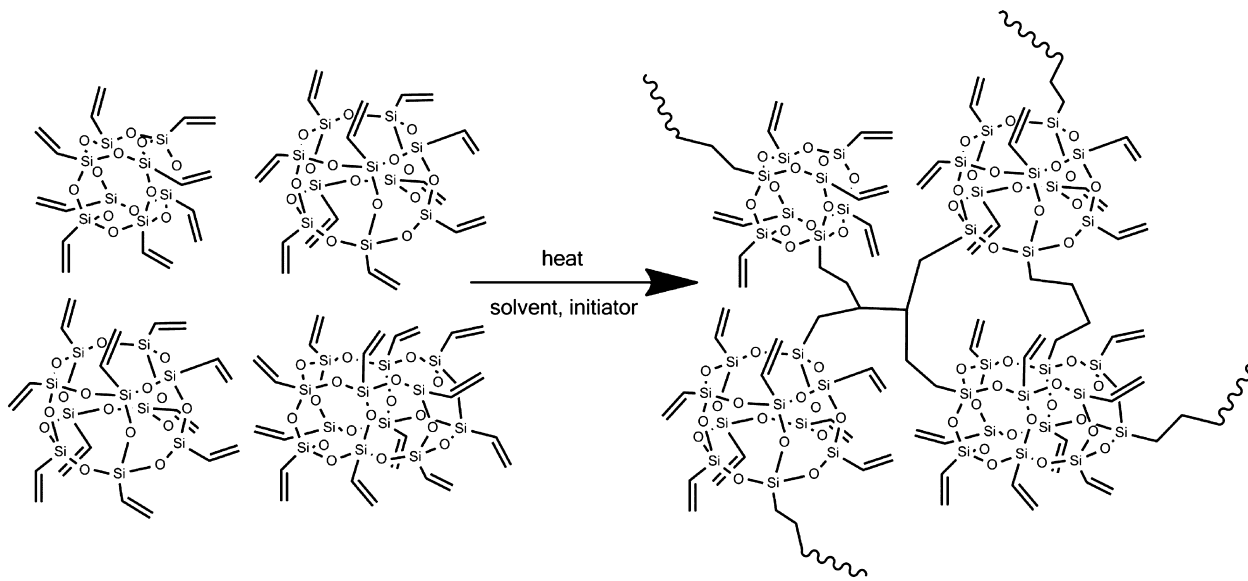
2.1. Materials. Polyhedral oligomeric vinylsilsesquioxane (vinylPOSS) cage mixture ($\text{RSiO}_{3/2}_n$, $n = 8, 10, 12$) with a nominal molecular weight of 633 – 950 Da was purchased from Hybrid Plastics, Inc. (Hattiesburg, USA) and used as received. Polyethyleneglycol (PEG) with an average molecular weight of 200 g mol^{-1} (PEG200) as well as azobisisobutyronitrile (AIBN) were purchased from Alfa Aesar (Karlsruhe, Germany). The other PEG standards came from Sigma Aldrich (Vienna, Austria). All other chemicals and solvents were purchased from Sigma Aldrich and used without further purification.

2.2. Apparatus. Fourier transform infrared spectroscopy (FTIR) spectra were measured with a Perkin-Elmer Spectrum 100 FTIR spectrometer. A Rayonet Chamber Reactor equipped with a cooling fan and placed in a thermostatted room at 13°C was used for photochemical reactions at an illumination wavelength of 253.7 nm . During photochemical reactions, the temperature inside the reactor was allowed to equilibrate, and reactions were therefore carried out at a constant reactor temperature of 22°C monitored with a thermometer inside the reactor. Thermally initiated polymerization was realized in a water bath thermostatted at 60°C for a fixed time of 24 h . Scanning electron micrographs were obtained using a Crossbeam 1540 XB scanning electron microscope (SEM) to probe the morphological and porous dry-state properties of the polymeric hybrid materials. Nitrogen adsorption/desorption isotherm measurements of dry bulk samples were performed with a Micromeritics TriStar II Surface Area and Porosity Instrument. Dry state surface areas were calculated from the Brunauer–Emmett–Teller (BET) model, while the mesopore size distribution was studied with the model of Barrett–Joyner–Halenda (BJH) from the adsorption branch of the isotherms.

2.3. Preparation of Materials and Postpolymerization Surface Modification. Respective vinylPOSS powder was first dissolved in a specific amount of porogenic solvent tetrahydrofuran (THF), and desired amounts of porogen PEG were added. This was done in a fashion that resulted in a constant weight fraction of $20\% \text{ (w/w)}$ hybrid vinylPOSS monomer mass to overall chemically inert porogenic solvent mixture of $80\% \text{ (w/w)}$ in all experiments. Typically, 16 wt \% AIBN (with respect to the vinylPOSS monomer mass) was added. The single-phase homogeneous liquid polymerization mixture was then filled in 4 mL glass vials for thermal polymerization. In some experiments the amount of AIBN was varied. The homogeneous liquid precursor solution was deoxygenated by bubbling through nitrogen for 5 min , followed by polymerization in the sealed vials at 60°C for 24 h in a water bath. After polymerization, the molded bulk polymers were cut into smaller pieces, washed with THF for 24 h in a Soxhlet apparatus, and dried in a vacuum oven at 40°C overnight.

2,2-Dimethoxy-2-phenylacetophenone (DMPA) was used to enhance efficiency for photochemical grafting reactions via thiol–ene “click” chemistry. Therefore, the monolithic materials were ground to an approximate millimeter size, and a dispersion of these materials in chloroform containing the respective thiol and initiator DMPA (1 wt \% with respect to the thiol) was subjected to stirring and UV

Scheme 1. Preparation of Organic–Inorganic Hybrid Polymers Based on Thermally-Initiated Free-Radical Polymerization of VinylPOSS Hybrid Precursors of the General Formula $(RSiO_{3/2})_n$ with $n = 8, 10, 12$ in Porogenic Diluents and Initiator



illumination in quartz glass vessels. To allow efficient thiol–ene addition, the concentration of thiol was adjusted to ensure excess toward residual vinyl groups of the scaffold. Therefore, 200 mg of pristine polymer was exposed to a solution of 500 mg of thioglycolic acid in 1 mL of chloroform containing 1 wt % of DMPA with respect to the thiol. This suspension was exposed to UV-irradiation under stirring. After modification, the materials were repeatedly washed with chloroform, THF, methanol, and THF, before drying in a vacuum oven followed by further characterization.

3. RESULTS AND DISCUSSION

3.1. General Properties of the Materials. Polyhedral vinylsilsesquioxane (vinylPOSS) precursor building blocks show a hybrid organic–inorganic structure and an absence of silanol groups (Scheme 1). It has been reported that this may lead to an improved pH tolerance for cage-like silsesquioxanes as compared to other silsequioxanes.²¹ In addition, the existence of a stable cage structure with a size of at least 1 nm and the multiplicity of tightly tethered short vinyl groups inherently leads to polymeric hybrid materials with an intrinsic nanoporosity since these can only pack with a limited density.^{20,30} These precursors can undergo vinyl polymerization with the reaction shown in Scheme 1. On the basis of preliminary experimental results, the vinylPOSS cage mixture ($(RSiO_{3/2})_n$ with $n = 8, 10, 12$, Scheme 1) shows an excellent solubility in THF. Initial experiments carried out using 20 wt % vinylPOSS in THF and 16 wt % AIBN with respect to the hybrid monomer mass in the precursor mixture, followed by free-radical polymerization, resulted in a transparent and glassy polymer (Figure 1). This polymer cracked on solvent evaporation and drying indicating a highly cross-linked structure. The fragile nature upon drying is explained by the high mechanical stress upon the 3D adhered, rigid, porous, and highly cross-linked structure of high porosity with very small pores and short covalent linkages between the precursors.

Figure 1 further demonstrates that replacing of specific weight fractions of THF with hydrophilic PEG200 shows a transition of the formed materials from transparent to increasingly opaque. This indicates a significant increase in pore sizes with respect to that of the POSS polymer prepared in

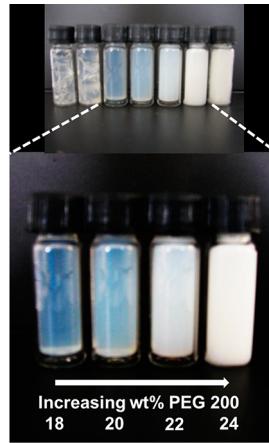


Figure 1. Visual appearance of the porous, monolithic polymeric hybrid materials derived from thermally initiated polymerization in a water bath at 60 °C for 24 h in the closed 4 mL glass vials. Porogenic solvent compositions are found in Table 1. From left to right: Polymer 2, Polymer 3, Polymer 4, Polymer 5, Polymer 6, Polymer 7, Polymer 8.

pure THF. Since PEG200 shows excellent solvent compatibility with THF, but is a poor solvent for the existent and hydrophobic vinylPOSS and its therefrom derived hybrid polymer in the polymerization mixture, this opacity consequently has its origin in the phenomenon of polymerization-induced phase separation. Therefore, larger pore sizes implied by a porogenic solvent, in which hybrid polymeric material in the relatively early stages of the polymerization reaction phase separates, may be expected (Figure 1). This is in agreement with what is typically observed in the preparation of monolithic polymeric adsorbents based on small organic precursors possessing desired functionality allowing scaffold formation. A poor solvent for the formed polymer nuclei/globule agglomerates leads to an earlier phase separation. It results in larger pore spaces in between the formed polymeric interadhered globule/nuclei agglomerates.¹⁴ The strongest change in opacity can be seen while moving from the 18 to 24 wt % PEG200 in the polymerization precursor mixture (Figure 1). Figure 2



Figure 2. Optical photographs and scanning electron microscopy images of selected hybrid materials. (a) Optical photographs of moldable porous monolithic material in 4 mL glass vials after polymerization and after cutting into smaller pieces, followed by Soxhlet extraction and drying in a vacuum oven overnight. The scanning electron microscopy images (b) and (c) show different magnifications to probe macro- and mesoporous properties. Left column: Polymer 5; Right column: Polymer 10.

shows that the monolithic material prepared from a 30 wt % PEG200 (Figure 2a, right image) appears as a white solid. Microscopically, the material shows large pores in between the hybrid, covalently attached globules (Figure 2b, right image) of which the macroscopically shaped and rigid material is composed. These globular structures are porous (Figure 2c, right image). However, while the large micrometer-sized pores are seen with 30 wt % PEG200 in the polymerization precursor mixture (Figure 2b, right image), they are absent at a weight fraction of 20 wt % PEG200 only (Figure 2b, left image). This indicates the occurrence of macrophase separation at increased weight fractions of PEG200.

Table 1 lists in detail the BET surface areas and observed BJH pore volumes for selected porogenic solvent compositions with the most interesting increments that show substantial differences in tailored mesopore volumes. It is striking that the pore volumes first increase from an initial $0.5 \text{ cm}^3/\text{g}$ for pure THF as porogenic solvent to achieve a maximum of $2 \text{ cm}^3/\text{g}$ at 22 wt % PEG200 in the polymerization precursor mixture. This is followed by descending mesopore volumes of materials at larger 22 wt % PEG200, a mixture composition that indeed stimulates formation of macropores. It correlates with the more pronounced opacity (Figure 1) and finally the appearance of large, micrometer-sized pores readily observable by SEM (Figure 2b). Larger pores contribute only very little to the observed pore volumes from nitrogen adsorption and consequently determined BET surface areas. The monolithic

Table 1. Impact of Porogenic Solvent Composition on Dry-State Surface Areas and Mesopore Volumes

material	porogenic solvent PEG/THF ^a	BET surface area (m^2/g)	Pore volume (cm^3/g) ^b
1	0/80	716	0.5
2	10/70	804	0.8
3	16/64	784	1.03
4	18/62	782	1.17
5	20/60	785	1.48
6	22/58	804	2.04
7	24/56	803	1.61
8	26/54	737	0.92
9	28/52	735	0.45
10	30/50	813	0.34
11	40/40	736	0.16

^aAll w/w, vinylPOSS 20% w/w. ^bBarrett–Joyner–Halenda (BJH) adsorption cumulative pore volume.

backbone with a finite, albeit small surface area stemming from the micrometer-sized through-pores, however, shows permanent and desired porosity. Since nitrogen adsorption/desorption analysis is not suitable to probe macroporous properties, clearly indicated by the visual appearance of the materials and SEM images (Figure 1, Figure 2), we subsequently reduce our discussion at this point to the nanoporous properties determined by the weight fraction of good solvent THF and PEG200 as porogenic diluents.

3.2. Impact of Porogenic Solvent Composition on Nanoporous Properties with Pore Sizes of 2–100 nm. Determination of nitrogen adsorption/desorption isotherms of the hybrid material derived with only THF as the pore-forming solvent reveals a type I physisorption isotherm⁴⁵ with a maximum volume of adsorbed nitrogen of $358 \text{ cm}^3/\text{g}$ (Figure 3a, filled squares). The nanoporous structure with only THF as pore-forming solvent having a BET surface area of larger than $700 \text{ m}^2/\text{g}$ is evident (Table 1). This is also demonstrated by the pore size distribution after BJH from adsorption data showing mesopores ($<10 \text{ nm}$) and indicating significant population of micropores of $<2 \text{ nm}$ (filled squares in Figure 3b). The inherent nanoporosity appears the most interesting feature of these materials and becomes determined by the alkyl-bridging frequency and distance between differently sized individual precursor blocks in the vinyl polymerization reaction (Scheme 1). It may be controlled by the termination rate of individual pendant vinyl radicals on the precursor with other vinylPOSS polymeric or monomeric precursors or initiator. Steric hindrance leave part of the vinyl groups inaccessible for polymerization (vide infra). On a nanoscale this must lead to heterogeneous networks. We believe that such heterogeneity is the major reason for the observed large surface area and relatively large pore sizes with respect to the vinylPOSS cage sizes (Scheme 1). It has already been indicated via other preparation methods that the effectiveness of cage linkage as well as linker lengths between cages can influence the observed nanoporous properties of related hybrid adsorbents.^{38,39,46}

Replacing specific amounts of PEG200 at the expense of THF in this scenario, to keep the weight fraction of vinylPOSS precursor against any porogenic diluent essentially constant, showed that the isotherms develop a pronounced hysteresis indicating a type IV physisorption isotherm⁴⁴ (e.g., half-filled circles in Figure 3a). Here, a maximum of the pore size distribution located at 9 nm could be clearly observed at a

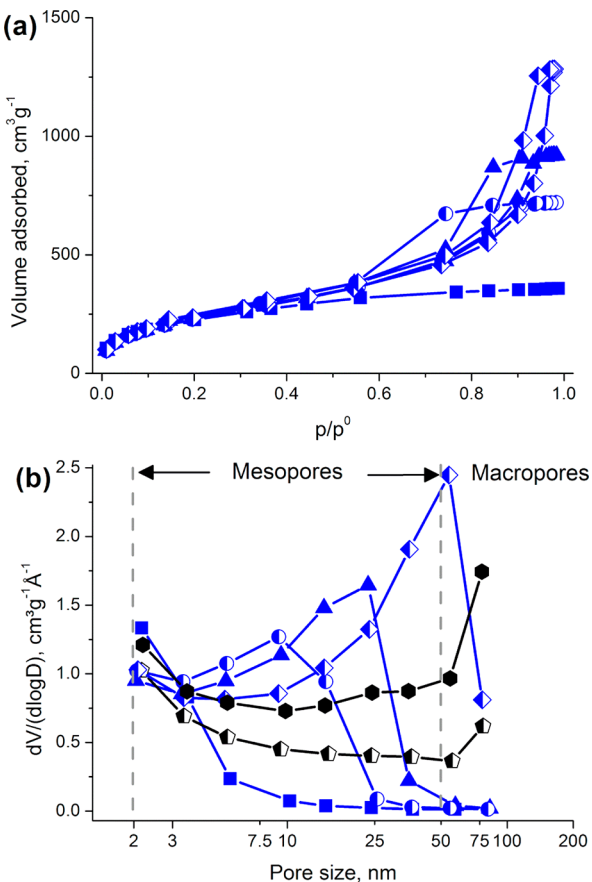


Figure 3. Impact of weight fraction of PEG200 employed as porogenic diluent component on the dry-state porous properties of vinylPOSS hybrid polymers. (a) Nitrogen adsorption/desorption isotherms of polymers 1, 4, 5, and 6 and (b) mesopore size distribution curves from adsorption according to Barrett-Joyner-Halenda of polymers 1, 4, 5, 6, 7, and 8. Symbols: Polymer 1 (filled squares), polymer 4 (half-filled circles), polymer 5 (filled triangles), polymer 6 (half-filled diamonds), polymer 7 (filled hexagons), polymer 8 (half-filled pentagons).

PEG200 weight fraction of 18 wt % (half-filled circles in Figure 3b). This is accompanied with a more than 2-fold increase in BJH pore volume from 0.5 to $1.2 \text{ cm}^3/\text{g}$, reflecting a significant population of mesopores with a certain distribution (Table 1, Figure 3). Upon further increase of the PEG200 weight fraction, a more distinct mesopore size distribution is observed (Figure 3b, filled triangles and half-filled diamonds). The strongest change in the mesoporous properties of the material with a defined maximum was observed between 10 and 22 wt % PEG200 in the polymerization precursor mixture. Within this compositional range, the mesoporous structure of the materials could be specifically influenced (Table 1 and Figure 3b). The maximum of the pore size distribution for a weight fraction of 22 wt % PEG200 in the polymerization mixture is located at 54 nm, and a maximum in the BJH pore volumes of a respectable $2 \text{ cm}^3/\text{g}$ was achieved (Table 1). This observed shift in pore sizes was in qualitative agreement with observations by SEM. Figure 4 shows SEM images of material bulk samples prepared in porogenic solvent containing a weight fraction of 20 wt % PEG200 (Figure 4a) and 22 wt % PEG200 (Figure 4b) with a maximum in the mesopore size distribution of 23 and 54 nm (Figure 3b). These results demonstrate the sensitive influence of porogenic solvent composition on the porous properties of the derived scaffolds.

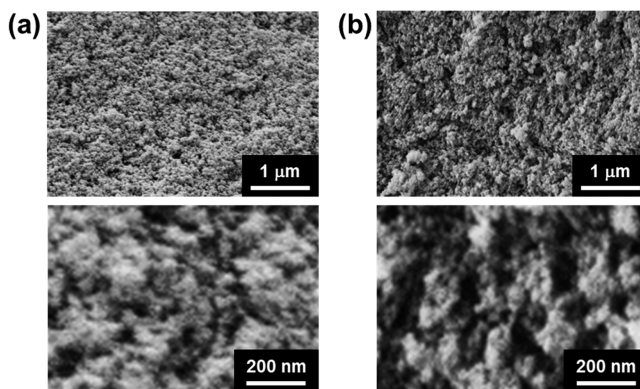


Figure 4. Scanning electron microscopy images of selected hybrid polymers with different magnifications in the upper and lower images indicating the increase in mesopore sizes in the structures. (a) Polymer 5 and (b) Polymer 6; for polymerization mixture compositions, please refer to Table 1.

Since the weight fraction of PEG200 had such a sensitive influence on the porous properties and the existence of a permanent nanoporous pore space, we also employed other polymeric porogens while keeping previous preparation parameters constant. PEG200 (20 wt %) was replaced by other polyethylene glycols including PEG600 in Figure 5a or PEG1000, or PEG3000, or PEG6000 in Figure 5b. Similarly to the different weight fractions of PEG200 in the polymerization precursor mixture, the chain length of the polymeric porogen impacts the porous properties. Using PEG600 as a polymeric porogen shows that the scaffold has macroporous properties, absent when using PEG200 at the same weight fraction (Figure 5a). This is a similar effect as if we would increase the PEG200 weight fraction (Figure 3b). The larger PEG porogens primarily induce formation of larger 100 nm sized macropores. Figure 6 then shows that selecting a PEG3000 polymeric porogen with much lower weight fractions of only 1–4 wt % in the polymerization precursor mixture allows tailoring of mesoporous properties. Further, PEG3000 primarily broadens the mesopore size distribution without pronounced maxima (Figure 6). These results therefore confirm the sensitive influence of the solvating properties of the constituents of the porogenic solvent mixture and their molecular weight that trigger polymerization-induced phase separation and pore space formation.

3.3. Impact of Initiator Concentration on the Porous Properties. All of the experiments reported so far were carried out at a constant initiator concentration of 16 wt % with respect to the vinylPOSS monomer mass. This is a relatively high initiator concentration in view of the initiators used in typical free-radical cross-linking polymerization processes to derive porous monolithic adsorbents. Therefore we also probed the impact of initiator concentration on the porous properties of the materials under the otherwise same conditions of polymerization temperature and time. Figure 7 clearly shows that the initiator concentrations only moderately influence the dry-state BJH pore size distribution when using only THF as pore-forming solvent (Figure 7a). In turn it is significant on the mesopore size distribution when employing PEG200 as a porogenic solvent component (Figure 7b). For example, a clearly defined maximum located at 15 nm could be observed for an initiator concentration of 4 wt % with respect to the vinylPOSS monomer mass (Figure 7b, filled triangles), while

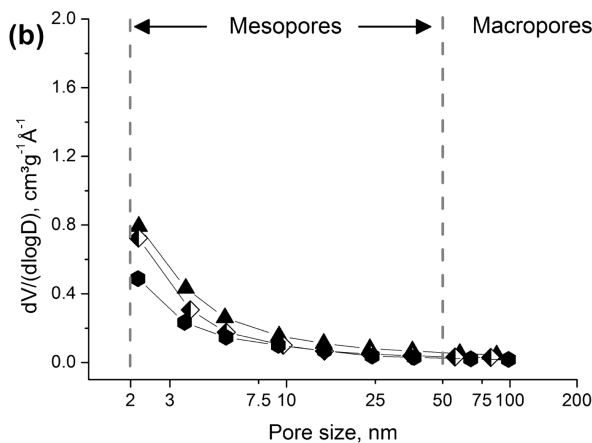
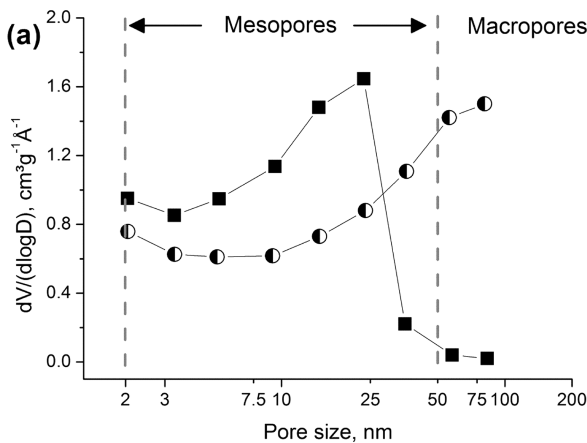


Figure 5. Impact of chain length of polymeric porogen at a weight fraction of 20 wt % (in analogy to Polymer 5) on the mesopore size distribution according to Barrett–Joyner–Halenda (BJH). (a) PEG200 and PEG600, and (b) PEG1000, PEG3000, and PEG6000. Symbols: PEG200 (filled squares), PEG600 (half-filled circles), PEG1000 (filled triangles), PEG3000 (half-filled diamonds), and PEG6000 (filled hexagons). Other preparation parameters are the same as in Table 1.

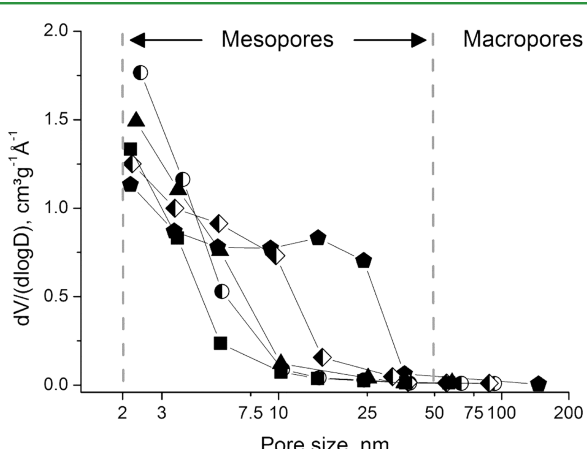


Figure 6. Impact of weight fraction of PEG3000 in the porogenic solvent mixture on the mesopore size distribution after Barrett–Joyner–Halenda. Symbols: THF (filled squares), 1 wt % PEG3000 (half-filled circles), 2 wt % PEG3000 (closed triangles), 3 wt % PEG3000 (half-filled diamonds), and 4 wt % PEG 3000 (filled pentagons). Other preparation parameters are the same as in Table 1.

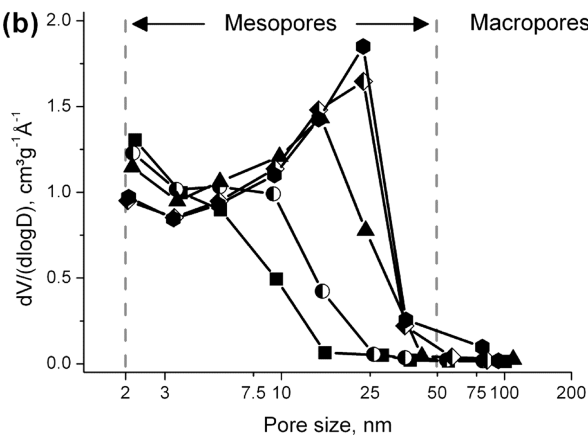
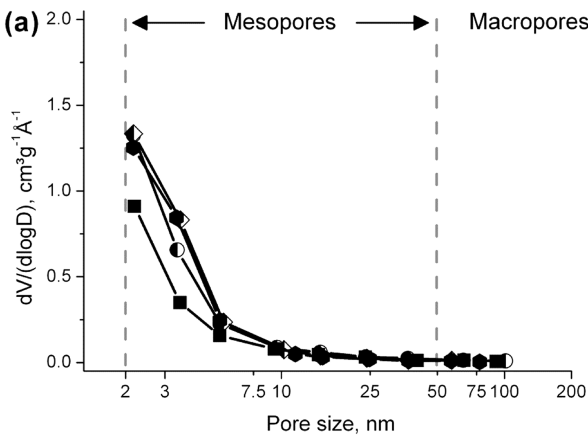


Figure 7. Impact of initiator concentration on the pore size distribution derived from adsorption according to Barrett–Joyner–Halenda referring to a mixture composition found in Table 1 for (a) Polymer 1 and (b) Polymer 5. Symbols: 1 wt % (filled squares), 2 wt % (half-filled circles), 4 wt % (filled triangles), 16 wt % (half-filled diamonds), 32 wt % (filled hexagons).

initiator concentrations below that value primarily created smaller-sized dry-state mesopore sizes. However, increasing initiator concentrations above 4 wt % resulted in a shift of the maximum of the pore size distribution toward 23 nm. At initiator concentrations in excess of 16 wt % with respect to the monomer mass, only an insignificant contribution to the dry-state pore volume, surface area, and maximum of the pore size distribution was observed (half-filled diamonds and filled hexagons). When using THF as the only pore-forming solvent (shown in Figure 7a), the inherent nanoporosity persists with only slightly decreasing pore volumes at initiator concentrations below 2 wt %.

These results demonstrate the increased degree of cross-linking (Scheme 1) and pore space rigidity of the materials prepared at increased initiator concentration in particular for mesopores (Figure 7b) and consequently reduced shrinkage after drying. This effect should be considered when using these materials for related engineering applications. The results also indicate that the vinylPOSS precursors show rather low vinyl group reactivity. This may be associated to poor reactivity of the tightly tethered vinyl groups to the silicon of the vinylPOSS cages.⁴⁰ Possible cage linkage proceeds through a distance only by a few carbon atoms which may be the reason for observing

microporosity and large surface areas.^{30,39,46} In our phase-separating system, it may additionally be associated to low diffusivity of the precursor (associated with their bulky, rigid molecular structure and high molecular weight). This makes diffusion the rate-limiting step for vinyl polymerizations including pore formation. The accessibility of reactive centers between already formed cage assemblies is increasingly diminished by the progression of the reaction and ad hoc explains the pertinent existence of pore sizes exceeding those expected from the densest possible packing. This may differ for polymerization systems employing varying linker length,^{38,39,44,46} potentially impairing observation of comparable surface areas.

3.4. From Meso- to Macroporous Properties. It is well-known that large interconnected pores enable excellent mass transfer by convection to the interactive or reactive sites immobilized in the porous structure that are accessible by diffusion. In particular, we observed that a PEG200 weight fraction ≥ 22 wt % leads to small macropores (>50 nm in size, Figure 3b). Their size could be further increased by simply increasing the PEG200 weight fraction in the polymerization precursor mixture, a condition that enables assessment of a range of pore sizes potentially enabling convective flow.^{14,19,20} Figure 8 shows the porous structure of bulk materials as probed

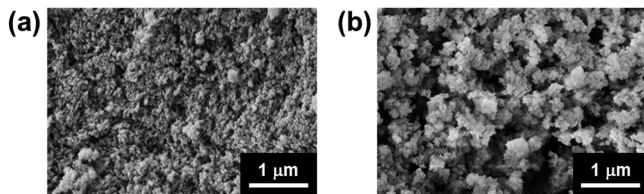


Figure 8. Scanning electron microscopy images of selected hybrid polymers showing the distinct development of macroporosity with (a) Polymer 6 and (b) Polymer 8. For polymerization mixture assignment please refer to Table 1.

by SEM and that were prepared at a weight fraction of 22 wt % PEG200 and 26 wt % PEG200. The existence of macropores at 26 wt % PEG200 could be evidenced (Figure 8b). Nitrogen adsorption analysis of materials prepared at larger 26 wt % PEG200 in the prepolymerization mixture indicates the subsequent decrease of mesopore volumes (Table 1). However,

the materials have a true hierarchy in porous properties (Figure 9) and total surface areas exceeding $700 \text{ m}^2/\text{g}$ (Table 1). The hierarchy becomes apparent due to the actual absence of a significant amount of pores in between 10 and 100 nm at a PEG200 wt % of ≥ 28 (filled triangles, half-filled circles, and filled squares in Figure 10). The porous properties as judged

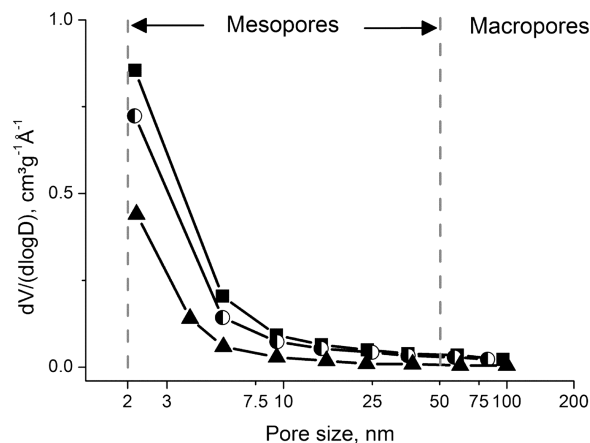


Figure 10. Pore size distribution after Barrett–Joyner–Halenda (BJH) for macroporous materials shown in Figure 9 to indicate their nanoporous properties. Increased weight fractions of macroporogenic diluent PEG200 subsequently increase the macropore size and reduce the amount and volume of nanopores. For polymerization mixture assignment, please refer to Table 1. Symbol assignment: Polymer 9 (filled squares), Polymer 10 (half-filled circles), Polymer 11 (filled triangles).

from SEM for a weight fraction of 28 and 30 wt % PEG200 appear similar to that obtained for macroporous polymer monoliths with a porous structure composed of globules¹⁹ together with a subsequent increase in globule size with a larger weight fraction of PEG200 in the porogenic diluent (Figure 9a and b). During this tailoring of large pores, however, the globular structures are porous as even indicated by SEM (Figure 9, lower row) and confirmed by nitrogen adsorption/desorption analysis (Table 1, Figure 10). The materials have mesopore volumes in a range of $0.34\text{--}0.45 \text{ cm}^3/\text{g}$ (Table 1) underlining their hierarchical structure composed of large convective transport pores and a multiplicity of small diffusive

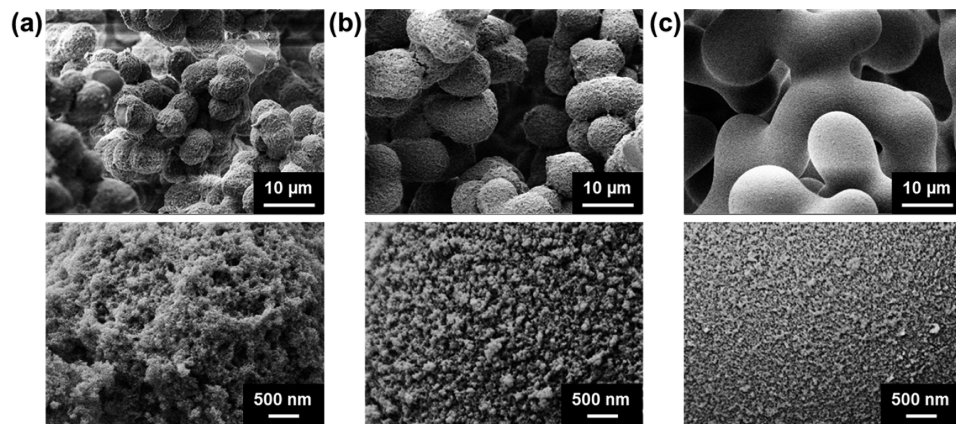


Figure 9. Scanning electron microscopy images of selected hybrid polymers with hierarchical pore structure composed of large micrometer-sized pores (upper images) and their mesoporous properties resulting in large surface areas indicated at a higher magnification (lower images). (a) Polymer 9, (b) Polymer 10, and (c) Polymer 11. For precursor mixture composition, please refer to Table 1.

pores. Moreover, further increase in the weight fraction of PEG200 results in a bicontinuous skeleton with a less coarse network structure and reduced amount of mesopore volumes (Figure 9c, Table 1).

3.5. Spectroscopic Characterization of Pristine Polymer. In view of later engineering applications, it appears desirable to tailor the mesoporous properties and thus gain a large surface area accessible by diffusion. Therefore, the materials should have the desired interacting, catalytic, or reactive functionality. All polymer samples with 20 wt % PEG200 in the polymerization mixture and prepared with varying initiator concentrations therefore underwent spectroscopic characterization with FTIR to show the impact of varying initiator concentrations on the apparently available residual vinyl groups. As can be seen in Figure 11, showing the

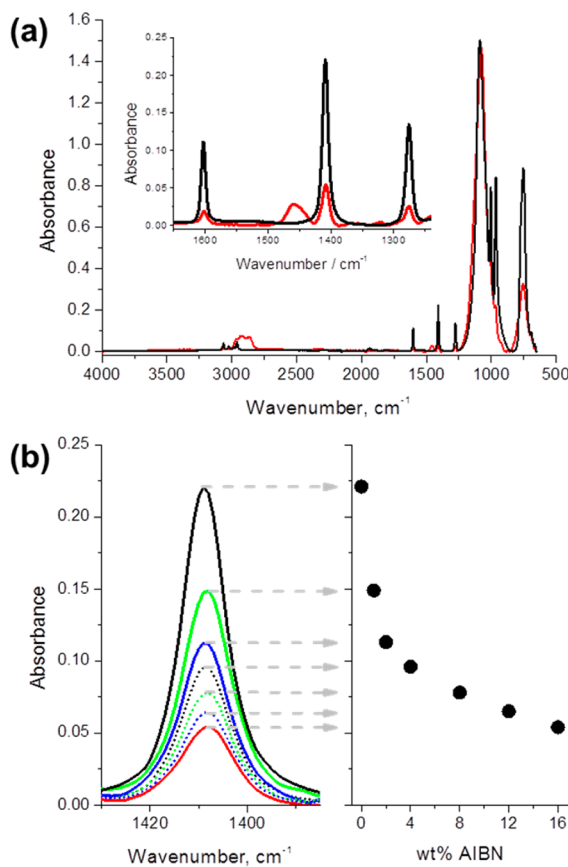


Figure 11. FTIR spectroscopy of polyhedral oligomeric vinylsilsesquioxane precursor and mesoporous organic–inorganic hybrid polymers (Polymer 5, Table 1) derived from varying initiator concentrations as indicated in the graph. (a) Normalized IR spectra in the range 500–4000 cm^{-1} and region of interest as inset with vinylPOSS precursor (black line) and hybrid Polymer 5 derived with 16 wt % initiator (red line) and (b) a decrease in normalized intensity of the vinyl group characteristic band at 1409 cm^{-1} with increased initiator concentrations used for preparation of Polymer 5. Dry-state mesopore size distributions of the materials can be found in Figure 7b.

most interesting bands associated with the vinyl groups, the material residual vinyl group content strongly correlated with the initial weight percentage of AIBN used for preparation. This is shown in more detail for the band at 1409 cm^{-1} (Figure 11b). We have seen earlier that the AIBN concentration significantly affects the material mesopore size distribution under otherwise identical preparatory conditions (Figure 7b).

This indicates that macroscopically rigid materials, whose mesopore space would not completely collapse upon drying, can be obtained at increased initiator concentrations. The most rigid materials were obtained with 16 wt % initiator. Further increases in initiator concentration did not contribute significantly to the development of higher dry-state mesopore volumes and associated surface areas (Figure 7b). The intensity of the peak at 1409 cm^{-1} shows a systematic decrease, reflecting a decrease in vinyl group content (Figure 11b) of the sample prepared at increased initiator concentrations. Similar trends have been indicated with the other bands as well (see Figure 11a). It indicates that a proper choice of initiator can balance porous properties and associated residual vinyl group content (Scheme 1). Both may be important for potential applications. While at an initiator concentration of 16 wt % approximately two residual vinyl groups (roughly estimated from the ratio of the vinyl group signal of the normalized FTIR spectra) remain in average for the polymerized vinylPOSS precursor material, it is more than five at an initiator concentration of 1 wt %. Though not being quantitative, the obtained results also show that even at very high initiator concentrations with respect to the vinylPOSS desirable pendant vinyl functionality of the scaffold is maintained. Future studies may show the impact of a balance between pore rigidity and swelling propensity as well as population of residual vinyl groups allowing chemical functionalization on the performance in model applications.

3.6. Modification via Thiol–Ene “Click” Chemistry. Thiol–ene “click” chemistry refers to a highly efficient route for the preparation of materials with desirable functionality and consequently controlled macromolecular architectures.^{47–49} Since our newly tailored and developed scaffolds contain a significant amount of pendant vinyl groups apparently not consumed in their preparation (Scheme 1, Figure 11) via a free-radical mechanism, we can then tailor internal functional properties with a facile grafting approach. This is schematically shown in Scheme 2. Grafting has been performed to ground

Scheme 2. Modification Strategy of Hybrid Polymers with Pendant Vinyl Functionality via Thiol–Ene “Click” Chemistry



monolithic materials suspended in chloroform containing the respective thiol and photochemical initiator in a UV-transparent reaction vessel under stirring and at controlled temperature of 22 °C. Following illumination with UV light, thiol radicals are generated as the first step of the reaction trajectory.⁴⁷ These add across the pendant carbon double bonds of the scaffold (Scheme 2) forming a carbon-centered radical intermediate. In conventional thiol–ene additions two mechanistic pathways may principally be possible from thereon. These are (i) hydrogen atom abstraction from another thiol or (ii) a homopolymerization with another equivalent of an “ene”.⁵⁰ Since in our scenario the “ene” functionality is tightly tethered on the scaffold and the grafting solution only contains thiols, chain transfer involving another existing thiol from the grafting solution completes thioether formation along with a new thiol radical. This route may link any desirable functional

moiety on the hybrid material via carbon–sulfur bond formation (Scheme 2), the key concept of the thiol–ene “click” chemistry.⁴⁸ The process is accelerated through the use of DMPA increasing the amount of reactive thyl radicals adding to the pendant double bonds on the scaffold.

To evidence the efficiency of this approach we prepared a series of thiol-modified materials with varying modification time on Polymer S (Table 1) prepared with only 1 wt % AIBN in the polymerization mixture and therefore having the largest amount of residual vinyl groups (Figure 11b). FTIR clearly reveals that the modification of these materials with thioglycolic acid is successful via the carbonyl absorption band located at 1710 cm⁻¹ (Figure 12a). Already after one minute, a significant amount of covalently attached moieties can be detected. The IR spectra further demonstrate an almost completion of the modification reaction after short periods of time, i.e., 10 min.

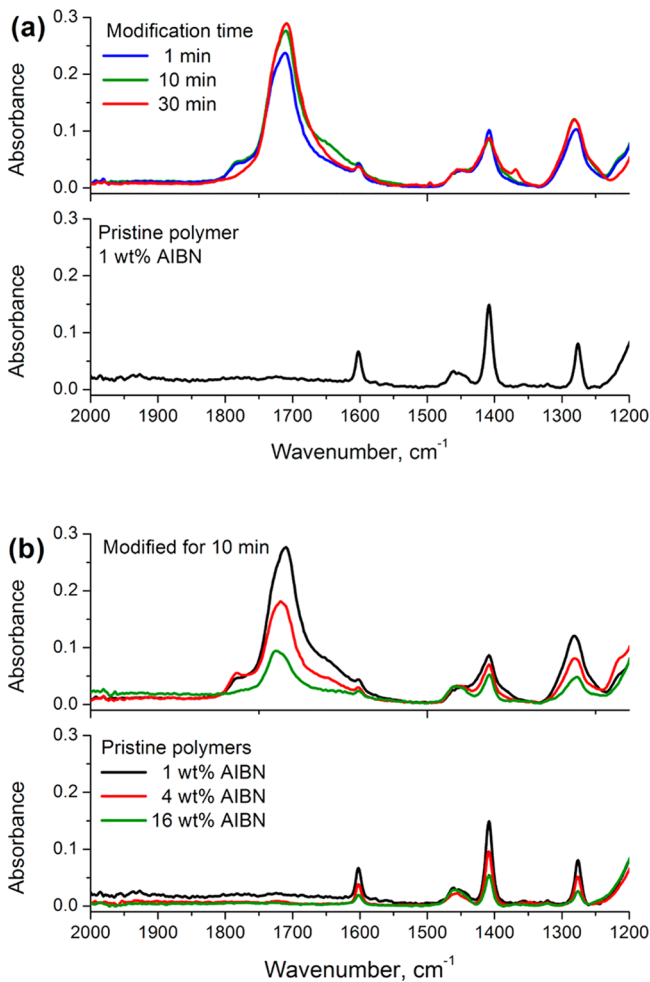


Figure 12. FTIR monitoring of the success of the thiol–ene “click” addition process at different times and vinyl group content of the porous material. (a) Normalized IR spectra of “click”-modified scaffolds prepared with Polymer S and derived with 1 wt % AIBN in the polymerization precursor mixture at different modification times of 1, 10, 30 min, and (b) normalized IR spectra of “click”-modified scaffolds at a fixed modification time of 10 min with pristine polymers prepared from 1, 4, and 16 wt % AIBN with respect to the monomer. The spectra clearly discern the thioglycolic acid features with characteristic bands for the carbonyl at 1711 cm⁻¹. Other bands associated with the bound thioglycolic acid are located at 1408 and 1280 cm⁻¹.

Additionally, we used this approach with polymers prepared at varying initiator concentrations and thus varying degrees of cross-linking and vinyl group content (Figure 7b, Figure 11). At a fixed modification time of 10 min and employing pristine polymers prepared from 1, 4, and 16 wt % AIBN (Figure 12b, lower traces), a greater amount of vinyl moieties that reacted with thioglycolic acid is detected for pristine materials prepared at the lower initiator concentrations (Figure 12b, upper traces). Thiol–ene “click” modification, therefore, represents a powerful tool for interface modification of residual vinyl groups on these porous scaffolds. Moreover, the high efficiency of the thiol–ene “click” reactions already at an advanced stage after just one minute of modification (Figure 12a), together with the spatial selective grafting ability in possible microfluidic or other applications, may represent the gate to highly useful and functional, large surface area porous scaffolds.

4. CONCLUSION

In summary, we describe a highly flexible route for the preparation of large surface area hybrid materials based on vinylPOSS utilizing a single-step molding process. Our approach provides the materials with desirable properties for related engineering applications with the option to tailor nanoporosity (in particular mesoporosity implying pore sizes of 2–50 nm) and macroporosity (implying pores sizes of ≥ 50 nm up to several micrometers) in a regime which also allows introduction of a distinct hierarchy in pore space. Experimental results show that the hybrid materials’ porous properties could be fine-tailored in hierarchical domains such as combining nanoporosity (microporosity, mesoporosity) and macroporosity. Furthermore, the versatility of this single type of precursor and the inherently tailorable amount of vinyl-pendant functionality enable interface decoration in the highly flexible context of thiol–ene “click” chemistry. This provides well-defined surface decoration without undesirable growth of polymer while introducing functionality, as for example realized via established radical grafting techniques.⁵¹ Although this type of interface modification has been demonstrated in the bulk, there is no roadblock for performing it in *in situ* flow through mode of the porous materials in microengineering devices. While these promising material characteristics, allowing for a separate optimization of the porous and interfacial properties, may emerge for a diversity of applications, we are currently working on the immobilization of suitable ligands for flow-through applications such as extraction, chromatography, or catalysis.

■ AUTHOR INFORMATION

Corresponding Author

*E-mail: ivo.nischang@jku.at. Tel.: + 43 (0) 732671547-66.

Author Contributions

[†]Both authors contributed equally to this work.

Notes

The authors declare no competing financial interest.

■ ACKNOWLEDGMENTS

This work was supported by the Austrian Science Fund (FWF) under project number [P24557-N19]. The authors would like to express gratitude to Andreas Schnölzer at the Institute of Polymer Chemistry, Johannes Kepler University Linz, for support of this study through initial help with the nitrogen

adsorption/desorption measurements. Günter Hesser at the Center for Surface and Nanoanalytics, Johannes Kepler University Linz, is acknowledged for experimental support with the scanning electron microscopy measurements.

■ REFERENCES

- (1) Svec, F.; Germain, J.; Frechet, J. M. J. *Small* **2009**, *5*, 1098–1111.
- (2) Svec, F.; Frechet, J. M. J. *Science* **1996**, *273*, 205–211.
- (3) Buchmeiser, M. R., Ed. *Polymeric Materials in Organic Synthesis and Catalysis*; Wiley-VCH: Weinheim, 2003.
- (4) Dioos, B. M. L.; Vankelecom, I. F. J.; Jacobs, P. A. *Adv. Synth. Catal.* **2006**, *348*, 1413–1446.
- (5) McKeown, N. B.; Budd, P. M. *Chem. Soc. Rev.* **2006**, *35*, 675–683.
- (6) Sachse, A.; Galarneau, A.; Coq, B.; Fajula, F. *New J. Chem.* **2011**, *35*, 259–264.
- (7) Anderson, E. B.; Buchmeiser, M. R. *Chem. Cat. Chem.* **2012**, *4*, 30–44.
- (8) Molnar, A. *Chem. Rev.* **2011**, *111*, 2251–2320.
- (9) Davis, M. E. *Nature* **2002**, *417*, 813–821.
- (10) Namera, A.; Nakamoto, A.; Saito, T.; Miyazaki, S. *J. Sep. Sci.* **2011**, *34*, 901–924.
- (11) Xu, L.; Shi, Z. G.; Feng, Y. Q. *Anal. Bioanal. Chem.* **2011**, *399*, 3345–3357.
- (12) Unger, K. K.; Ditz, R.; Machtejevas, E.; Skudas, R. *Angew. Chem., Int. Ed.* **2010**, *49*, 2300–2312.
- (13) Tanaka, N.; Kobayashi, H.; Nakanishi, K.; Minakuchi, H.; Ishizuka, N. *Anal. Chem.* **2001**, *73*, 420A–429A.
- (14) Svec, F.; Frechet, J. M. J. *Chem. Mater.* **1995**, *4*, 707–715.
- (15) Svec, F.; Tennikova, T. B.; Deyl, Z. *Monolithic materials: preparation, properties, and applications*; Elsevier: Amsterdam, 2003.
- (16) Viklund, C.; Svec, F.; Frechet, J. M. J.; Irgum, K. *Chem. Mater.* **1996**, *3*, 744–750.
- (17) Okay, O. *Prog. Pol. Sci.* **2000**, *25*, 711–779.
- (18) Andrzejewska, E. *Prog. Polym. Sci.* **2001**, *26*, 605–665.
- (19) Nischang, I.; Brueggemann, O.; Svec, F. *Anal. Bioanal. Chem.* **2010**, *397*, 953–960.
- (20) Nischang, I.; Brueggemann, O.; Teasdale, I. *Angew. Chem., Int. Ed.* **2011**, *50*, 4592–4596.
- (21) *Applications of Polyhedral Oligomeric Silsesquioxanes*; Hartmann-Thompson, C., Ed.; Springer: New York, 2011.
- (22) Cordes, D. B.; Lickiss, P. D.; Rataboul, F. *Chem. Rev.* **2010**, *110*, 2081–2173.
- (23) Kickelbick, G. *Prog. Polym. Sci.* **2003**, *28*, 83–114.
- (24) Sanchez, C.; Soler-Illia, G. J. D. A.; Ribot, F.; Lalot, T.; Mayer, C. R.; Cabuil, V. *Chem. Mater.* **2001**, *13*, 3061–3083.
- (25) Roll, M. F.; Asuncion, M. Z.; Kampf, J.; Laine, R. M. *ACS Nano* **2008**, *2*, 320–326.
- (26) Choi, J.; Yee, A. F.; Laine, R. M. *Macromolecules* **2003**, *36*, 5666–5682.
- (27) Gnanasekaran, D.; Madhavan, K.; Reddy, B. S. R. *J. Sci. Ind. Res.* **2009**, *68*, 437–464.
- (28) Marcolli, C.; Calzaferri, G. *Appl. Organomet. Chem.* **1999**, *13*, 213–226.
- (29) Harrison, P. G.; Kannengiesser, R. *Chem. Commun.* **1996**, 415–416.
- (30) Zhang, C. X.; Babonneau, F.; C. Bonhomme, C.; Laine, R. M.; Soles, C.-L.; Hristov, H. A.; A. F. Yee, A. F. *J. Am. Chem. Soc.* **1998**, *120*, 8380–8391.
- (31) Laine, R. M. *J. Mater. Chem.* **2005**, *15*, 3725–3744.
- (32) Morrison, J. J.; Love, C. J.; Manson, B. W.; Shannon, I. J.; Morris, R. E. *J. Mater. Chem.* **2002**, *12*, 3208–3212.
- (33) Pielichowski, K.; Njuguna, J.; Janowski, B.; Pielichowski, J. *Adv. Polym. Sci.* **2006**, *201*, 225–296.
- (34) Zhang, L.; Abbenhuis, H. C. L.; Yang, Q. H.; Wang, Y. M.; Magusin, P.; Mezari, B.; van Santen, R. A.; Li, C. *Angew. Chem., Int. Ed.* **2007**, *46*, 5003–5006.
- (35) Caro, J.; Noack, M. *Microporous Mesoporous Mater.* **2008**, *115*, 215–233.
- (36) Kumar, P.; Gulants, V. V. *Microporous Mesoporous Mater.* **2010**, *132*, 1–14.
- (37) Chaikittisilp, W.; Sugawara, A.; Shimojima, A.; Okubo, T. *Chem.—Eur. J.* **2010**, *20*, 6006–6014.
- (38) Roll, M. F.; Kampf, J. W.; Kim, Y.; Yi, E.; Laine, R. M. *J. Am. Chem. Soc.* **2010**, *132*, 10171–10183.
- (39) Kim, Y.; Koh, K.; Roll, M. F.; Laine, R. M.; Matzger, A. J. *Macromolecules* **2010**, *43*, 6995–7000.
- (40) Wang, Z. B.; Leng, S. W.; Wang, Z. G.; Li, G. Y.; Yu, H. *Macromolecules* **2011**, *44*, 566–574.
- (41) Qin, Y.; Ren, H.; Zhu, F.; Zhang, L.; Shang, C. W.; Wie, Z. J.; Luo, M. M. *Eur. Polym. J.* **2011**, *47*, 853–860.
- (42) Peng, Y.; Ben, T.; Xu, J.; Xue, M.; Jing, X. F.; Deng, F.; Qiu, S. L.; Zhu, G. S. *Dalton Trans.* **2011**, *40*, 2720–2724.
- (43) Guo, H.; Meador, M. A. B.; McCorkle, L.; Quade, D. J.; Guo, J.; Hamilton, B.; Cakmak, M.; Sprowl, G. *ACS Appl. Mater. Interfaces* **2011**, *3*, 546–552.
- (44) Lin, H.; Ou, J.; Zhang, Z.; Donga, J.; Zou, H. *Chem. Commun.* **2013**, *49*, 231–233.
- (45) Sing, K. S. W.; Haul, R. A. W.; Moscou, L.; Pierotti, R. A.; Rouquerol, J.; Siemieniewska, T. *Pure Appl. Chem.* **1985**, *57*, 603–619.
- (46) Hoebbel, D.; Endres, K.; Reinert, T.; Pitsch, I. *J. Non-Cryst. Solids* **1994**, *176*, 179–188.
- (47) Hoyle, C. E.; Bowman, C. N. *Angew. Chem., Int. Ed.* **2010**, *49*, 1540–1573.
- (48) Hoyle, C. E.; Lowe, A. B.; Bowman, C. N. *Chem. Soc. Rev.* **2010**, *39*, 1355–1387.
- (49) Lowe, A. B. *Polym. Chem.* **2010**, *1*, 17–36.
- (50) Northrop, B. H.; Coffey, R. N. *J. Am. Chem. Soc.* **2012**, *134*, 13804–13817.
- (51) Ranby, B.; Yang, W. T.; Tretinnikov, O. *Nucl. Instrum. Methods Phys. Res., Sect. B* **1999**, *151*, 301–305.